J. Biochem. 2011;150(5):553–562 doi:10.1093/jb/mvr099

JB THE JOURNAL OF BIOCHEMISTRY

Mapping of NRF binding motifs of NF-kappaB p65 subunit

Received June 20, 2011; accepted July 11, 2011; published online August 5, 2011

Marc R. Reboll[1], Aike T. Schweda[2], Myriam Bartels[3], Raimo Franke[1], Ronald Frank[1] and Mahtab Nourbakhsh[1,*]

[1]Department of Chemical Biology, Helmholtz Centre for Infection Research, Inhoffenstraße 7, D-38124 Braunschweig; [2]Institute for Molecular- and Cellphysiology; and [3]Institute of Pharmacology, Hannover Medical School, D-30625 Hannover, Germany

*Mahtab Nourbakhsh, Collaborative Research Centre SFB 566, Hannover Medical School, Carl-Neuberg-Straße 1/OE 6790, 30625 Hannover, Germany. Tel: +49 5341 8862733, Fax: +49 531 6181 3499, email: mnourbakhsh@hotmail.com

NF-kappaB repressing factor (NRF) is a nuclear transcription factor that binds to a specific DNA sequence in NF-kappaB target promoters. Previous reports suggested that NRF interferes with the transcriptional activity of NF-kappaB binding sites through a direct interaction with NF-kappaB subunits. The aim of this study was to map specific NRF binding domains in the NF-kappaB proteins, p65 and p50. Our data demonstrate that NRF is able to interact with the p65 subunit and inhibit its transcription enhancing activity in reporter gene experiments. Using tandem affinity purifications (TAP), we show that NRF protein significantly binds to the endogenous p65, subunit but not to the p50 subunit. The selective binding activity of the NRF protein is consistently mediated by the N-terminal domain of NRF (Amino acids 1–380). Moreover, the Rel homology domain (RHD) of p65 is sufficient for binding to the N-terminal domain of NRF. Using detailed peptide mapping studies, we finally identify three peptide motifs in p65 RHD showing distinctive binding specificities for the NRF protein. According to the predicted structure of p65, all three peptide motifs align within an exposed region of p65 and might hint at promising targets for inhibitors.

Keywords: NF-kappaB/NRF/peptide array/protein–protein interaction/transcriptional regulation.

Abbreviations: CBP, calmodulin binding peptide; CREB, cAMP response element binding protein; HDAC1, histone deacetylase 1; IFN-b, interferon beta; IL-1, Interleukin-1; IL-8, Interleukin-8; iNOS, inducible nitric oxide synthase; NRE, negative regulatory element; NRF, NF-kappaB repressing factor; PMA, phorbol 12-myristate 13-acetate; PPI, protein–protein interaction; RHD, Rel homology domain; TAD, transcription activation domain; TAP, tandem affinity purification; TEV, tobacco etch virus; TFIID, transcription factor IID.

The family of NF-kappaB transcription factors responds to diverse cell stimuli by activating the expression of stress response genes. Multiple signals, including cytokines and bacterial and viral products, induce NF-kappaB transcriptional activity (*1*). Five polypeptides, p50, p65, c-Rel, p52 and RelB, constitute the entire NF-kappaB family, and these proteins share an N-terminal Rel homology domain (RHD). The RHD consists of an N-terminal folded domain of 160–210 amino acids, a short flexible linker of ~10 amino acids and a C-terminal folded domain roughly spanning 100 (*2*). All NF-kappaB subunits can form various homo- and hetero-dimer combinations via their RHDs. Theoretically, the formation of 15 homo- and heterodimers is possible from the five NF-kappaB subunits (*3*); however, only 12 could be identified *in vivo* (*2*). The predominant form is the p65-p50 heterodimer, which assembles with a significantly greater stability than either of the respective p50-p50 or p65-p65 homodimers (*4*). The positions Asp-256 and Tyr-269 in p50 symmetrically associate with positions Asn-200 and Phe-213, respectively, in p65 and stabilize the heterodimer through hydrogen bonds at the interface (*2*). Besides dimerization, the RHD is responsible for sequence-specific DNA binding and nuclear localization as well as interaction with the inhibitors of kappaB proteins (IkappaBs) (*5*). Only three NF-kappaB subunits, p65, c-Rel and RelB, contain a transcription activation domain (TAD) bordering their RHD domains at the C-terminal end. The TAD is responsible for the transcriptional activation of NF-kappaB target genes. Consequently, NF-kappaB dimers that possess at least one of these subunits can act as transcriptional activators (*6*).

NF-kappaB repressing factor (NRF) is a nuclear transcription factor that is constitutively expressed in variable amounts in all human tissues (*7*). Using an inducible NRF antisense expression approach in human epithelial cells, NRF was implicated in the basal silencing of NF-kappaB target genes, including interferon beta (IFN-b) and inducible nitric oxide synthase (iNOS) (*7*). Additional studies on HIV-1 long terminal repeat (LTR) and Interleukin-8 (IL-8) promoters revealed that NRF is also required for transcriptional activation upon specific stimulation with phorbol 12-myristate 13-acetate (PMA) or Interleukin-1 (IL-1) (*8*, *9*). It was therefore suggested that endogenous NRF plays a dual role in gene transcription in concert with other accessory co-factors. Detailed characterization of NRF revealed that the N-terminal domain of NRF, spanning amino acids 1–296, inhibits the transcriptional activity of NF-kappaB binding sites in

reporter gene experiments (*7*). Recently, down-regulation of NRF was associated with elevated NF-kappaB activity in cystic fibrosis and pancreatic cancer (*10*, *11*). Here, we report that NRF exclusively interacts with the NF-kappaB subunit p65. Additionally, we define three NRF-binding peptide sequences in p65 RHD close to the p50 interaction domain.

Material and Methods

Plasmid constructions

p65 and pLexA expression plasmids were described earlier (*7*). The NdeI/BamHI fragment of the p65 expression plasmid was removed to create the (p65RHD) expression plasmid. The vector pLexA-p65 was constructed by transferring a HindIII/EcoRI fragment encoding LexA from pLexA into the p65 plasmid. The reporter plasmid pL6NLuc was derived from pL6 (*7*). After the insertion of the NRF binding site (NRE) next to the LexA site in this vector, the CAT reporter gene was replaced by firefly luciferase from pTA-Luc (Clontech) using the PvuI/EcoRI sites. NRF–TAP expression plasmids were described previously (*12*). Expression plasmids pNRF(1–380) and pNRF(1–690) carrying NRF and linker sequences were obtained by inserting stop codons in the corresponding TAP vectors. The control vector pRL-Tk was obtained from Promega. The NRF-Strep expression plasmid (pEXPR-NRF-Strep) was created by the insertion of a PvuI/blunted BamHI fragment encoding full length NRF from NRF(1–690)TAP into pEXPR-IBA103 (IBA). For additional controls of the peptide mapping experiments, the vectors pEXPR-IBA105 (IBA) and pEXPR-JKTBP1 (*13*) were used to express the strep tag and Strep-JKTBP1 *in vitro*, respectively.

In vitro expression of proteins

The NRF-Strep expression plasmid (pEXPR-NRF-Strep) as well as the control vectors pEXPR-IBA105 and pEXPR-JKTBP1 were added to the *in vitro* expression kit TNT obtained from Promega to express NRF-Strep and control proteins. The reactions were performed according to manufacturer's instructions.

The pNRF(1–690)TAP and p65 expression plasmids were added to the *in vitro* expression kit TNT obtained from Promega together with [^{35}S]methionine to express radioactive proteins. The reactions and the determination of protein concentration were performed according to manufacturer's instructions. The radioactive labelled proteins served as standards for protein concentration in TAP experiments.

Peptide mapping

The p65 RHD peptide arrays were generated by the SPOT-synthesis technique, as described earlier (*14*). Briefly, peptides were synthesized on an amino-functionalized cellulose membrane using Fmoc/*tert*-butyl chemistry. The spots consist of ~5 nmol of each peptide (*15*). For the binding assays, the peptide arrays were blocked overnight at room temperature with blocking buffer consisting of 2× blocking buffer concentrate (Sigma-Genosys Inc., #B6429) and 5% (w/v) sucrose in TBS-T [0.02 M sodium phosphate buffer with 0.15 M sodium chloride (pH 7), 0.05% Tween 20]. Approximately 1 μg of NRF-Strep protein in blocking buffer was added to p65 RHD peptide arrays for 4 h at room temperature. Next, the arrays were washed with a 10-fold volume of TBS-T three times and then incubated with AP-conjugated streptavidin (Calbiochem, #189732). Finally, a chemiluminescence reaction (Biorad, #170-5018) was performed to detect the bound fraction of NRF-Strep protein.

Cell lines and transfection

HeLa (CCL-2, LGC Promochem) cells were maintained in DMEM with 5% FCS. For reporter assays, the cells were transfected by calcium phosphate coprecipitation (*16*). A total of 6 μg of reporter and expression plasmids together with 0.5 μg of a *Renilla* expression plasmid were transfected per 7.5×10^4 cells. After 48 h, the cells were harvested and pooled for reporter gene assays. Firefly and *Renilla* luciferase activities were determined using the Dual-Luciferase reporter system (Promega Corporation) as described in the manufacturer's protocol. Luciferase activity was measured in a Lumat LB 9501 luminometer (Berthold). For TAP-purification, HeLa cells were transfected with indicated NRFTAP expression plasmids by calcium phosphate precipitation.

TAP purification

The TAP purification was performed as described (*17*) with the following modifications. HeLa cells were transfected with either TAP or NRF–TAP fusion protein- encoding plasmids. Forty-eight hours later, the cells were stimulated with IL-1 (10 ng/ml) for 3 h were indicated. Approximately 10^8 cells were lysed in buffer A [10 mM HEPES/KOH (pH 7.9), 10 mM KCl, 1.5 mM $MgCl_2$, 5 mM DTT, 0.1% Nonidet P-40, 0.3 mM Na_3VO_3, 20 mM glycerol-2-phosphate, 10 μM protease inhibitor E64, 2.5 μg/ml leupeptin, 0.3 mM PMSF, 1 μM pepstatin, 400 μM okadaic acid (pH 7.9)]. Equal aliquots of cellular extracts were used for Western blot analysis using α-p65 antibody or α-p50 antibody (sc8008, sc8414, Santa Cruz Biotechnology) and peroxidase antiperoxidase soluble complex antibody produced in rabbit (PAP, Sigma-Aldrich) to confirm equal expression of TAP fusion proteins. Equal amounts of cellular extracts were incubated with IgG-agarose (Sigma-Aldrich Inc., Munich, Germany) in salt-adjusted buffer A (150 mM NaCl) at 4°C overnight to bind TAP-tagged proteins. Following three washing steps with wash buffer [10 mM Tris (pH 8.0), 150 mM NaCl and 0.1% Nonidet P-40], the binding of TAP fusion proteins to equal aliquots of IgG-agarose (10%) was examined by western blot analysis using peroxidase anti-peroxidase soluble complex antibody produced in rabbit (PAP, Sigma-Aldrich). Complexes were released from IgG-agarose by TEV-protease (30 U; Invitrogen Life Technologies) in TEV buffer [10 mM Tris–HCl (pH 8.0); 150 mM NaCl, 0.1% Nonidet P-40, 1 mM DTT, 0.5 mM EDTA, 1 μM protease inhibitor E64]. Complexes containing calmodulin binding peptide (CBP)-tagged proteins were immobilized on a calmodulin affinity resin (Stratagene) for 4 h at 4°C. Complexes were washed

five times with CBP buffer [50 mM Tris–HCl (pH 8.0); 150 mM NaCl, 1 mM Mg-acetate, 1 mM imidazole, 10 mM 2-ME, 2 mM $CaCl_2$]. Finally, 20 µl of gel loading buffer (*9*) was added to the bound protein complexes and incubated for 10 min at 65°C. The samples were subjected to SDS gel electrophoresis together with protein concentration standards (*9*). Western blot analysis was performed using a mouse monoclonal antibody against p65 (sc8008) or p50 (sc8414) and secondary goat anti-mouse antibody (sc2005) from Santa Cruz Biotechnology. The dissociation constant K_d for NRF and p65 in TAP experiments was estimated according to the equation described for immobilized proteins earlier (*18*). The concentrations of NRF–TAP and p65 in input and bound fractions were estimated using densitometric analysis of protein standards and detected signals.

Western blot analysis

Western blots were performed as described earlier (*9*). TAP fusion proteins were detected using peroxidase anti-peroxidase soluble complex antibody produced in rabbit (PAP, Sigma-Aldrich). Antibodies against p65 (sc8008) and p50 (sc8414) were obtained from Santa Cruz Biotechnology.

Results

Reporter gene analysis demonstrates the functional interaction of p65 and NRF

We have previously shown that NRF represses the transcriptional activity of NF-kappaB binding sites (*7*), which can theoretically bind the 12 known different sets of NF-kappaB dimers. Here, we first attempted to characterize the functional interaction of p65 and NRF in HeLa cells. Therefore, we used the reporter plasmid pL6NLuc, comprising firefly luciferase coding sequences under the control of a DNA-binding element for the *Escherichia coli* LexA protein (LexA) and the NRF binding sequence from the human IL-8 promoter [negative regulatory element (NRE)]. This reporter was transfected into HeLa cells together with a constitutively active *Renilla* luciferase expression vector as an internal transfection control. Additionally, the pLexA-p65 vector encoding a fusion protein of the N-terminal LexA DNA binding domain and the C-terminal full-length p65 protein was transfected. As shown in Fig. 1, the LexA-p65 fusion protein leads to transcriptional activation of the reporter and significantly high expression of firefly luciferase. Additional expression of two different NRF proteins spanning amino acids 1–380 [pNRF(1–380)] or amino acids 1–690 [pNRF(1–690)] clearly decreases the firefly luciferase reporter gene expression. We observed slight differences in inhibition between NRF(1–380) and NRF(1–690). This might be based on the previously reported partial nucleolar localization of overexpressed NRF(1–690) (*19*), which might constrain its mobility and transcriptional activity. Nevertheless, full-length NRF and its N-terminal domain are both able to inhibit the transcriptional enhancing activity of the LexA-p65 protein.

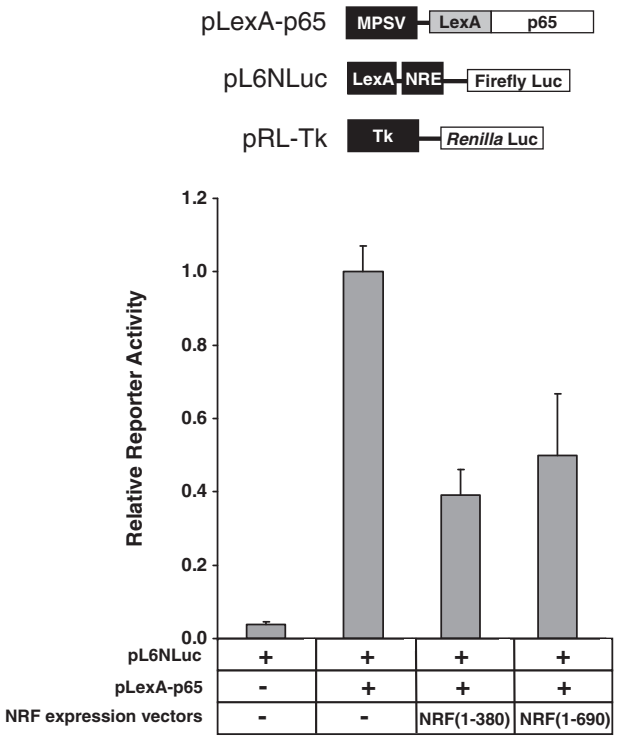

Fig. 1 NRF inhibits the transcriptional activity of p65 protein. A schematic diagram of the transfected vectors is shown at the top of diagram. pLexA-p65 contains an MPSV promoter (MPSV) as well as the coding sequences of the LexA DNA binding domain and the p65 full length protein. pL6NLuc encodes firefly luciferase as a reporter gene. Its expression is controlled by a LexA site, containing six LexA binding motifs, and a NRF binding site (NRE). Additionally, NRF-encoding plasmids pNRF(1–380) and pNRF(1–690) were transfected. pRL-Tk served as an internal control comprising a thymidine kinase promoter (Tk) and the *Renilla* luciferase gene (*Renilla* Luc). HeLa cells were transfected with the vectors pLexA-p65, pL6NLuc, internal control vector pRL-Tk and pNRF(1–380) or pNRF(1–690), where indicated. Two days after transfection, the cells were harvested and the luciferase activities were determined. Firefly luciferase activities were compared to the corresponding *Renilla* luciferase activities to calculate the relative firefly luciferase activity, shown here as the mean + SD of three transfection experiments. The relative firefly luciferase activity of cells transfected with pL6NLuc and pLexA-p65 was set to 1.

NRF does not bind p50 *in vivo*

To study the specificity of NRF and p65 interaction in cells, we used NRF–tandem affinity purification (TAP) fusion proteins (Fig. 2A). This TAP tag involves two affinity tags, CBP and IgG binding domains of protein A, separated by a specific tobacco etch virus (TEV) protease cleavage site. The two consecutive affinity purification steps provide a more stringent purification of interacting proteins compared to a single step procedure (*17*). Three different NRF–TAP fusion proteins as well as the TAP tag alone were transiently expressed in HeLa cells. NRF(1–690)TAP is composed of the NRF full-length protein and the C-terminal TAP tag. Fusion proteins NRF(1–380)TAP and NRF(1–149)TAP contain NRF amino acids 1–380 and 1–149, respectively. These mutants were initially constructed based on an isolated partial cDNA coding for amino acids 1–380 or by using a single restriction site (EcoRI) present in the NRF coding sequence

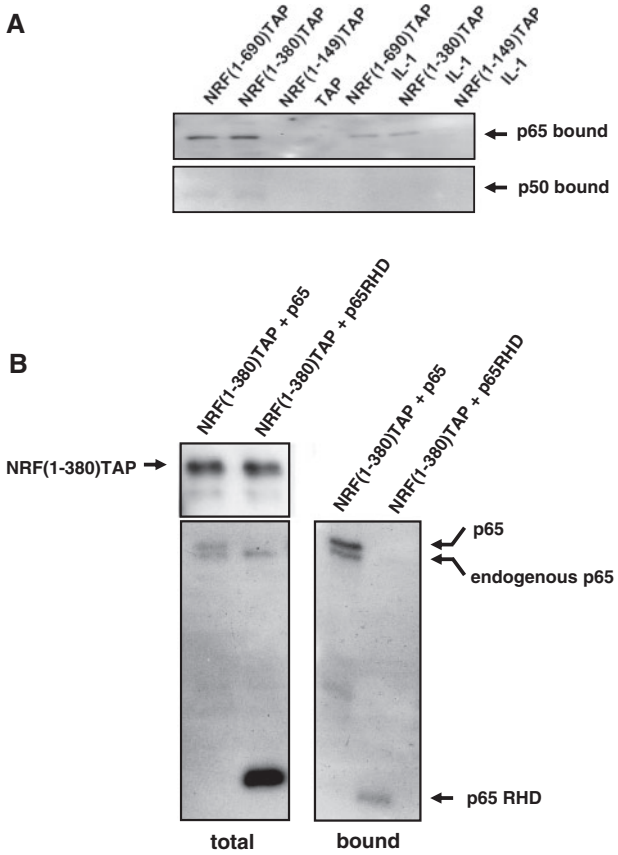

Fig. 2 NRF binds to endogenous p65 but not to p50. (A) HeLa cells were transfected with equal amounts of expression plasmids encoding NRF1–690TAP, NRF1–380TAP, NRF1–149TAP or TAP tag alone. Two days after transfection, the cells were stimulated with IL-1 (10 ng/ml) for 3 h where indicated. Cellular extracts were prepared, and the amount of p65 and p50 was detected by Western blot (Supplementary Fig. S1). Next, equal aliquots of the cellular extracts were incubated with IgG-agarose. After several washing steps, 10% of the bound fraction of the TAP fusion proteins was monitored by western blot (Supplementary Fig. S1). Following TEV digestion and the subsequent second purification step, the amounts of p65 and p50 were monitored by western blotting and marked as bound p65 and p50. (B) HeLa cells were transfected with equal amounts of expression plasmids encoding NRF1-380TAP, with either p65 or p65 RHD. TAP analysis and detection were performed as described in section (A). Western Blot analysis of total NRFTAP, total p65 proteins and bound p65 proteins is shown and proteins are indicated by arrows.

(amino acids 1–149). Thus, NRF(1–149)TAP contains a nuclear localization signal (NLS) but lacks the DNA binding domain that is present in NRF(1–380)TAP (*7*). Finally, cellular extracts were first tested for equal amounts of p65 or p50 as a control (Supplementary Fig. S1, total p65 or p50) and subjected to TAP analysis later. Cellular lysates were incubated with IgG-agarose for the first step of purification. Following several wash steps, the samples were tested for an equal level of bound TAP fusion protein by western blot analysis (Supplementary Fig. S1, total TAP fusion proteins). IgG-agarose was then incubated with TEV to split off the bound protein A domains. For the second purification step, the supernatants were added to calmodulin beads. Finally, the amounts of the transcription factors p65 and p50 were detected in each bound protein fraction by western blot analysis (Fig. 2A). The data show that NRF1-690TAP and NRF1-380TAP are able to interact with the endogenous p65 protein (Fig. 2A, p65 bound). The amount of NRF1-690TAP and p65 proteins in input and bound fractions was estimated using radioactive labelled NRF1-690TAP and p65 protein standards. Based on the estimated concentrations, we calculate a dissociation constant of 10^{-8} M for NRF1-690TAP and p65 proteins (data not shown). In comparison, NRF1-149TAP and the TAP tag fail to bind to p65. Strikingly, p50 barely binds to either NRF1-690TAP or NRF1-380TAP fusion proteins. NRF and p65 were previously found to be involved in the transcriptional activation of the IL-8 promoter upon IL-1 stimulation (*8*). Therefore, we analysed whether IL-1 treatment might affect the interaction of p65 or p50 with NRF. Importantly, upon IL-1 treatment of cells (Fig. 2A, +IL-1), the endogenous p65 shows a lower binding affinity to NRF. However, p50 fails to bind to NRF either before or during IL-1 stimulation. Thus, independent of IL-1 stimulation, NRF seems to specifically interact with the p65 but not the p50 subunit *in vivo*.

NRF (1–380) interacts with p65 RHD *in vivo*

To assess the binding of p65 RHD to the N-terminal domain of NRF, we cotransfected the NRF1-380TAP expression vector and the full-length p65 or truncated p65 RHD expression vectors into HeLa cells (Fig. 2B). The equal expression of NRF1-380TAP fusion protein was tested by western blot analysis. The p65 antibody is a mouse monoclonal antibody raised against amino acids 1–286 of human p65 that detects the endogenous and overexpressed p65 as well as the p65 RHD in cellular lysates (Fig. 2B; total). TAP experiments reveal that overexpressed p65, endogenous p65 and the truncated p65 RHD bind to amino acids 1–380 of NRF (Fig. 2B; bound). This is in agreement with the previous observation that a short central domain of NRF (amino acids 204–308) binds to p65 RHD (*12*). The presence of p65 RHD in cellular extracts leads to apparent decrease of p65 binding to NRF (Fig. 2B, bound). This might be due to a preferential formation of p65 to p65 RHD heterodimers with a possible lower affinity to NRF. On the other hand, the signal intensities of p65 and p65 RHD strongly depend on the antibody binding affinity and the blotting characteristics of each single protein as well. Therefore, it is rather difficult to estimate and compare the NRF binding affinities of p65 and p65 RHD in these experiments.

NRF-Strep binds to three short domains in p65 RHD

We used the previously described SPOT technique (*20*) to identify the p65 RHD amino acid sequences binding to NRF. In this approach, 15-mer peptides derived from the p65 RHD sequence were chemically synthesized by the SPOT method (*21*) and immobilized on a cellulose membrane. As shown in Fig. 3A, adjacent peptides share a common sequence of 12 amino acids but differ by 3 amino acids at the C- or N-terminal ends. Rabbit reticulocyte lysates (RRL) were used to rapidly express a relatively high concentration (120 nM) of the NRF-Strep fusion protein compared

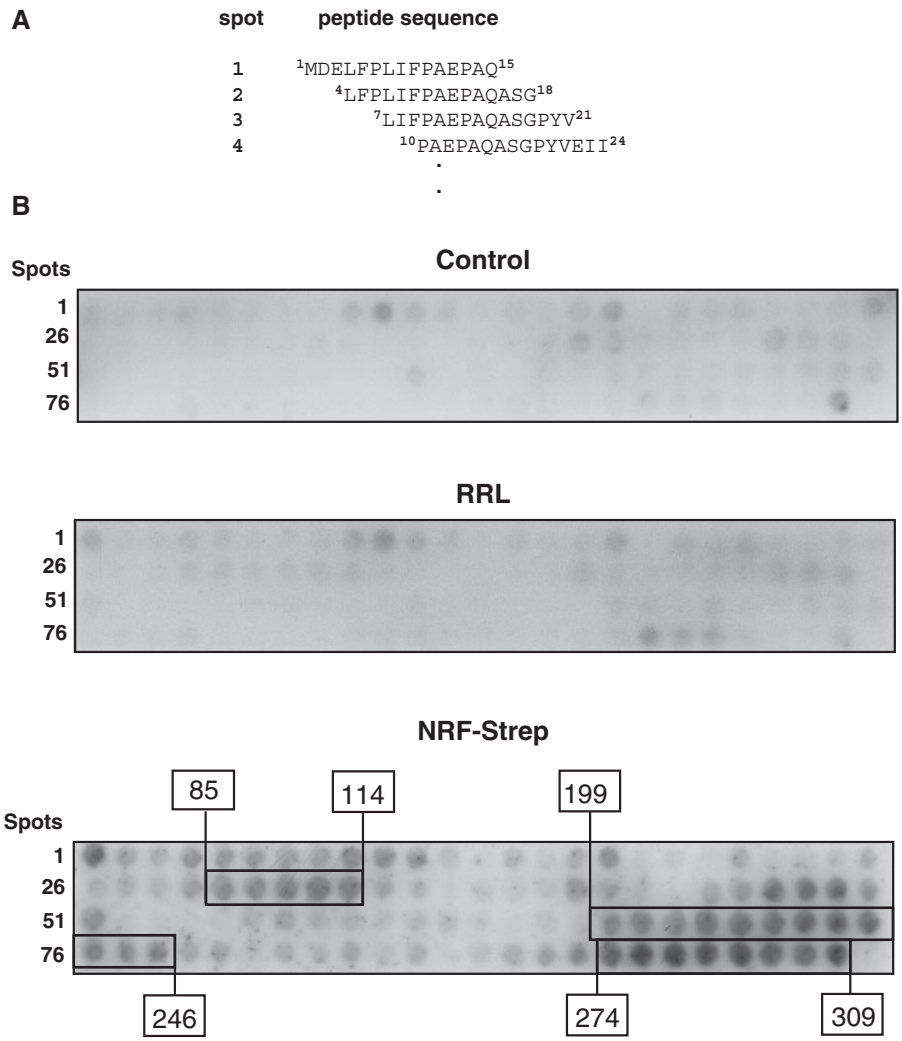

Fig. 3 Mapping of NRF binding sequence in p65 RHD. (A) The design of the array of 15-mer peptides corresponding to the p65 RHD protein sequences is shown. The superscripted numbers in the amino acid sequences correspond to p65 amino acids. (B) NRF-Strep fusion protein was expressed in rabbit reticulocyte lysates (RRL) and was incubated with the peptide array. The membrane was washed three times, and the binding of NRF-Strep protein was detected by streptavidin and subsequent chemiluminescence reaction (NRF-Strep). The first spot of each lane is indicated at the left. As controls, the peptide array after incubation with streptavidin alone (control) and after incubation with RRL lacking NRF-Strep and streptavidin (RRL) is presented. Three peptide motifs were identified after incubation with NRF-Strep and are indicated by the frames. The amino acid boundaries of each motif corresponding to the amino acids of the p65 RHD protein sequence are indicated at the top and bottom of the array.

to cell culture expression systems. Fusion of a C-terminal Strep tag to the NRF coding sequence allows specific detection of NRF protein bound to 15-mer peptides by streptavidin. Figure 3B shows that NRF-Strep fusion protein binds to three distinct peptide motifs (Fig. 3B, NRF-Strep). As a control, incubation with streptavidin without (Fig. 3B, control) or with RRL lacking NRF-Strep protein (Fig. 3B, RRL) revealed barely detectable background signals. We performed additional control experiments using the strep tag or Strep-JKTBP1 (*13*), and they showed no significant affinity to the p65 peptide spots (Supplementary Fig. S2). Together, this indicates that the NRF-Strep protein binds predominantly to 3 amino acid motifs corresponding to p65 amino acids 85–114 (motif 1), 199–246 (motif 2) and 274–309 (motif 3) respectively. Motifs 1 and 3 represent short protein domains spanning 30 and 35 amino acids, respectively. Motif 2 with 47 amino acidsresidues reaches over a relatively large central part of p65.

Further analysis of p65 RHD *amino acids*motifs

We performed additional peptide array experiments to further refine the mapping of the NRF binding domain in p65. The results in Fig. 3 indicate that motif 1 has a lower binding affinity to NRF protein compared to motifs 2 and 3. For Motif 1, we used a sizing approach that allows for the successive downsizing of binding sequences. As shown in Fig. 4A, 8- to 15-mer peptides corresponding to motif 1 were immobilized on a cellulose membrane. The stepwise single amino acids extension of the peptide length from 8 to 15 amino acids allows the precise mapping of a minimal binding motif. Adjacent peptides share an expanding common sequence from 7 to 14 amino acids but differ by a single amino acid at the C- or N-terminal ends.

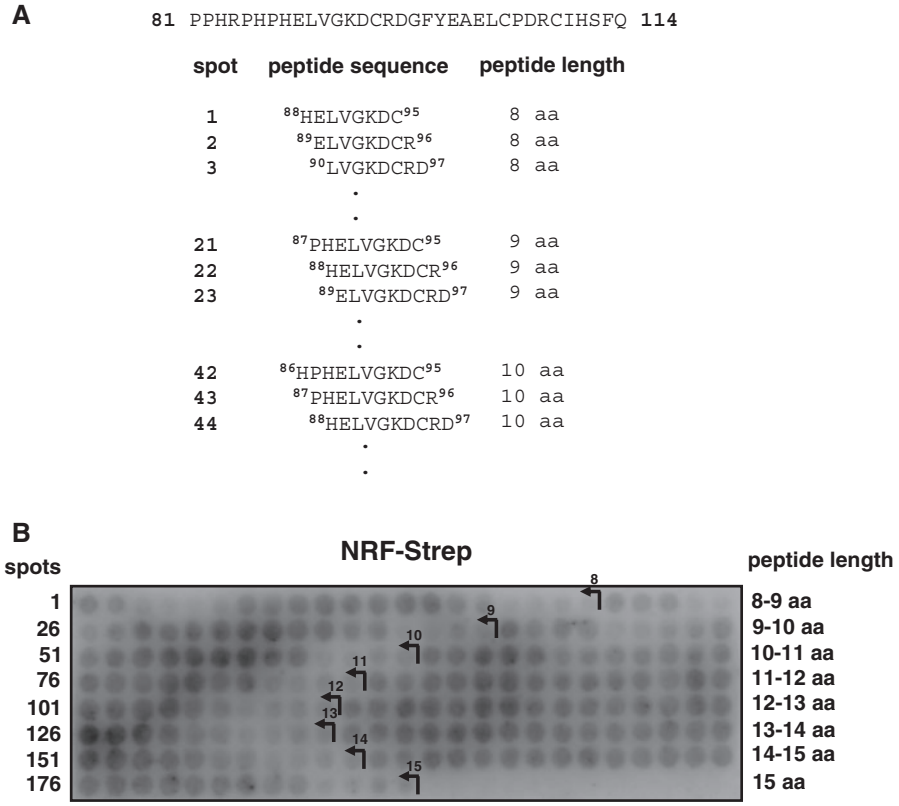

Fig. 4 Analysis of peptide motif 1 by a sizing approach. (A) The design of the array composed of peptides with varying sequence length is presented. The peptides are derived from p65 RHD amino acids 81–114. The superscripted numbers in amino acid sequences correspond to p65 RHD amino acids. (B) NRF-Strep protein was incubated with the peptide array and detected as described in the legend of Fig. 3B. Different peptide lengths are indicated by arrows on the membrane and on the right. Additionally, the first spot of each lane is indicated on the left.

The binding procedure was performed as described above. The control shows no affinity to streptavidin (Supplementary Fig. S3A). Following densitometric analysis, the signal intensities were classified into four groups: background, weak, strong and very strong signals (Supplementary Fig. S4). Accordingly, we searched for peptide sequences that predominantly occur in spots showing strong and very strong signals. The amino acid motif YEAELCPD (amino acids 100–107) was present in 36 spots of the peptides, mainly showing strong and very strong signals (72%). Moreover, a higher number of positive spots contained the core sequence AELC. For instance, motifs AELCPD lacking the first or YEAELC lacking the last two amino acids were found in 68 spots (Supplementary Fig. S4). Thus, we believe that the YEAELCPD motif might be involved in the NRF-p65 interaction.

For Motif 2, we used another approach to isolate a possible binding motif for NRF. Based on the length of Motif 2, we expected two separated binding motifs. In this case, the length of the immobilized peptides was kept constant. As depicted in Fig. 5A, adjacent peptides share a common sequence of 14 amino acids but differ by a single amino acid at C- and N-terminal ends. The binding procedure was performed as described above. Again, no positive signals were obtained with streptavidin (Supplementary Fig. S3B). Strikingly, NRF-Strep binds to all immobilized peptides but reveals a significantly higher signal intensity with peptides containing the C-terminal end of motif 2 (Fig. 5B). Therefore, we suggest that amino acids 224–246 might be involved in the binding of p65 to NRF-Strep protein.

In Fig. 3, motif 3 (amino acids 274–309) shows the strongest affinity to NRF-Strep. For further isolation of interacting amino acids, we used an alanine scan approach. Therefore, 15-mer peptides corresponding to motif 3 were synthesized and immobilized on a single array. As shown in Fig. 6A, adjacent peptides differ by a single amino acid substitution by alanine. The first 16 peptides correspond to amino acids 274–288 of p65. Following a blank spot, the next 16 peptides correspond to amino acidsa 277–291 of p65, and each carry a single alanine substitution. Following the binding procedure, all peptides are able to bind to NRF-Strep (Fig. 6B). Note that blank spots contain no peptides as an additional control, and the control spots show negligibly low background binding of streptavidin (Supplementary Fig. S3C). We performed a densitometric analysis of the detected signals (summarized in Supplementary Figure S5). Although none of the amino acid exchanges to alanine cause a complete loss of NRF-Strep binding, several exchanges significantly decrease the signal intensity. The most prominent reduction was detected after substitution of glutamic acid 279 with alanine (E279A). Glutamic acid is negatively charged and located at an exposed position within a loop structure in p65 RHD (Fig. 7B). Therefore, it is

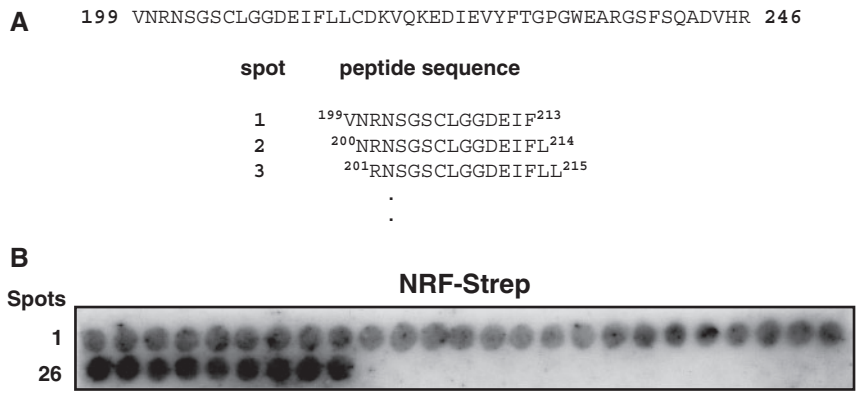

Fig. 5 Peptide scan of motif 2. (A) The setup of the array of 15-mer peptides corresponding to p65 RHD amino acids 199–246 is shown. The superscripted numbers in amino acid sequences correspond to p65 RHD amino acids. (B) NRF-Strep protein was incubated with the peptide array and detected as described in the legend of Fig. 3B. The first spot of each lane is indicated on the left.

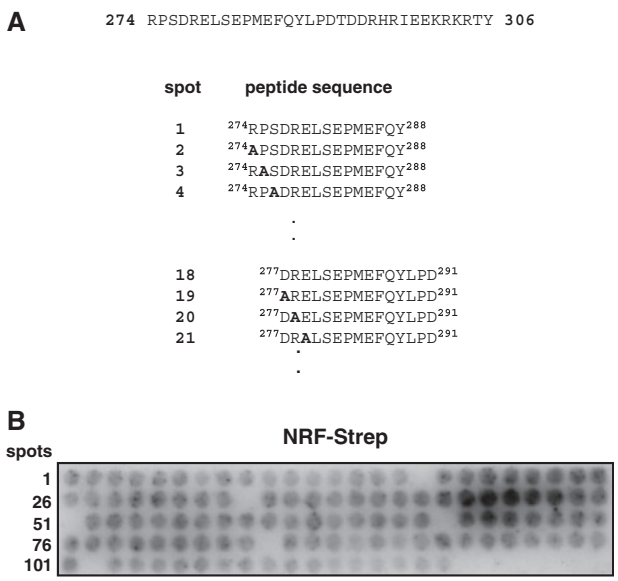

Fig. 6 Alanine scan of motif 3. (A) The design of the 15-mer peptide array corresponding to p65 RHD amino acids 274–306 is shown. The superscripted numbers in the amino acid sequences correspond to p65 amino acids. (B) NRF-Strep protein was incubated with the peptide array and detected as described in the legend of Fig. 3B. The first spot of each lane is indicated at the left.

conceivable that the substitution of glutamic acid with the neutral amino acid alanine can affect the binding of NRF-Strep to this motif.

Taken together, we have identified three peptide sequences in p65 RHD with distinctive binding affinities for NRF protein. Thus, these peptides might represent the anticipated sites of NRF-p65 interaction and can possibly be used as small interfering peptides.

Discussion

Protein–protein interactions (PPIs) are the fundamental basis for many crucial regulatory networks, and mapping PPIs at every scale is the key to identifying new targets for therapeutic strategies. We have previously reported that NRF directly interacts with NF-kappaB p65 protein to regulate the IL-8 gene in human epithelial cells (*8*, *12*). Recently, NRF was implicated in aberrant NF-kappaB activity in cystic fibrosis and pancreatic cancer, the latter being one of the most lethal and treatment-resistant forms of cancer (*10*, *11*). Thus, mapping NRF and NF-kappaB interactions may lead to new strategies for therapeutic intervention against these diseases.

In general, different sets of NF-kappaB homo- and heterodimers are able to bind to the NF-kappaB DNA binding consensus sequence (GGGRNNYYCC) (*22*). X-ray structure analysis of the NF-kappaB consensus sequence in complex with NF-kappaB homo- and hetero-dimers revealed that two subunits are required to encircle the target DNA (p50/p65 heterodimer, Fig. 7B) (*23*). The LexA reporter assay in our study monitors LexA-p65 transcription activity independent of its binding to the NF-kappaB consensus sequence. The assembly of LexA-p65 proteins led to a significant increase in reporter gene expression. According to previous reports, this is based on the p65 TAD (*24*). Full-length NRF or the N-terminal domain of NRF (1–380) interferes with the transcriptional activity of LexA-p65 TAD. This is in agreement with our previous reports showing that NRF inhibits the transcription-enhancing activity of adjacent NF-kappaB binding elements (*8*, *12*). Furthermore, the TAP co-purification experiments in Fig. 2 confirm a selective interaction between NRF–TAP and p65 in cellular extracts that contain both p65 and p50 subunits in excess (Supplementary Fig. S1). A negligible amount of p50 was rarely detected in the bound fraction, which might be due to a partial co-purification of p50 by binding to p65. Nevertheless, a direct interaction between p50 and NRF seems very unlikely.

Previously, NRF was shown to differentially act on the activation of the IL-8 gene by NF-kappaB upon IL-1 stimulation in human epithelial cells (*8*, *10*, *11*). Our data indicate that the binding of p65 to NRF is attenuated upon IL-1 stimulation. Therefore, we suggest that the differential regulation of the IL-8 promoter in IL-1 stimulated cells might be at least partially due to the disparate mode of NRF and p65

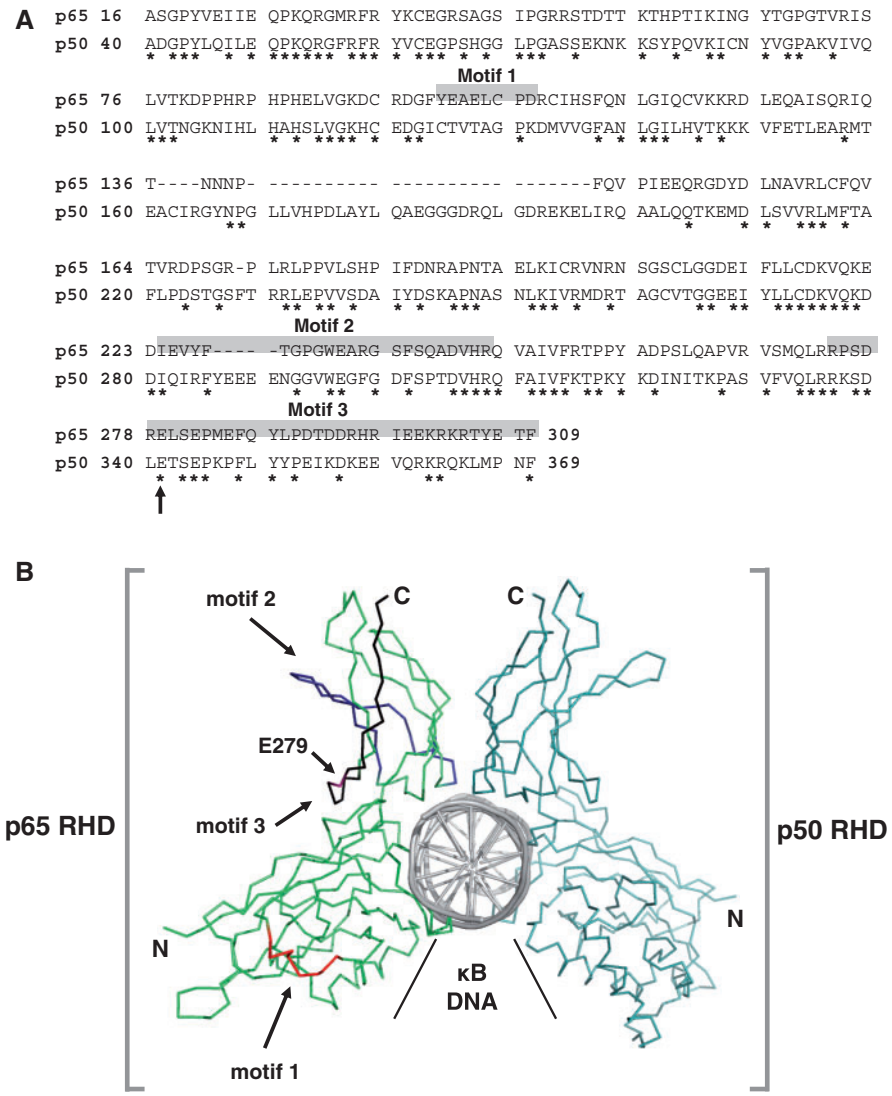

Fig. 7 NRF interacting motifs in p65 RHD sequence and structure. (A) The comparison of the p65 RHD (NP_068810.3) and p50 RHD (NP_003989.2) sequences is shown. The alignment was performed using the blastp tool at http://www.ncbi.nlm.nih.gov/. Homologous amino acids are indicated with an asterisk. NRF binding motifs are highlighted in grey. Amino acid E279 is indicated by an arrow at the bottom. (B) The protein structure of the p65 RHD-p50 RHD complex bound to DNA (PDB ID: 2I9T) is presented using PyMol software (*32*). The three NRF binding motifs in p65 RHD are depicted and indicated by arrows. Amino acid E279 is highlighted in purple and indicated by an arrow. The N- and C-terminus of each protein is indicated as well.

interaction or to IL-1 mediated phosphorylation of p65 as reported earlier (*25*).

Further characterization of the NRF binding domain reveals that p65 RHD is able to bind to the N-terminal domain of NRF. In addition, we utilized a set of different antibodies including histone deacetylase 1 (HDAC1) (*23*), cAMP response element binding protein (CREB) binding protein (*26*) and transcription factor IID (TFIID) (*27*) to examine the binding of a variety of p65 binding co-factors to NRF. However, none of these cellular co-factors were able to bind to the NRF–TAP fusion protein (data not shown). Thus, p65 remains the only known transcription factor that binds to NRF so far.

Previous studies have shown that p65 and p50 proteins interact via their RHDs sharing 41% sequence homology (Fig. 7A). Together with the data presented here, we suggest that p65 RHD is able to bind to both NRF and p50. Notably, NRF and p50 reveal no significant sequence homology. Thus, it is tempting to speculate that both p50 and NRF bind to different sequence motifs in p65 RHD. In fact, the slight co-purification of p50 together with p65 bound to NRF (in Fig. 2A) might hint at a potential common complex of p50, p65 and NRF, the existence of which remains to be proven experimentally.

The further isolation of NRF binding domains in p65 protein reveals three distinct peptide motifs within the RHD. Motif 1 is exclusively found in p65 RHD and not in p50 RHD; it seems to be highly specific for NRF binding. The 72% of peptides containing this motif strongly bind NRF. Importantly, the 51 peptides that were missing the entire or part of motif 1 in this experiment failed to bind NRF protein. In

comparison, motif 2 spans 23 amino acids, and its C-terminal domain (amino acids 224–246) has an especially strong binding affinity for NRF protein. Although we cannot explore a core sequence in motif 2, we find an exceptional gap of 5 amino acid residues in this motif by comparison of p50 and p65 RHDs. Thus, these additional residues might be responsible for the selective binding of NRF. Motif 3 shows the highest binding activity for NRF and seems to interact with NRF over its entire length. Only a single mutation, E279A, could significantly reduce the binding of NRF, down to 30% (Supplementary Fig. S5).

X-ray structures of individual NF-kappaB dimers revealed a new mode of DNA recognition wherein a dimer composed of RHDs intimately contacts the major groove of the NF-kappaB target DNA sequence (*28*, *29*). We aligned the three identified NRF binding motifs in the predicted structure for the p65 RHD/p50 RHD dimer (*23*). Most importantly, we find the entire length of all three motifs on the surface of the p65 protein in complex with p50 RHD and DNA (Fig. 7B and Supplementary Fig. S6). Interestingly, the N-terminal region of motif 2 contains amino acid residues 200 and 213, which approach p50 RHD to form a p50/p65 heterodimer. Although NRF shows an average binding to the N-terminal tail of motif 2, we believe that the binding of NRF to p65 might at least affect the formation of p50/p65 heterodimers. However, extensive studies will be required to confirm this hypothesis. Given that elevated p65 activity has a causative function in inflammation and transformation (*30*, *31*), the identified motifs might be valuable targets for new therapeutics.

Supplementary Data

Supplementary Data are available at *JB* Online.

Acknowledgements

The authors thank Susanne Daenicke and Birgit Ritter for excellent technical assistance and Werner Tegge for helpful discussions.

Funding

Deutsche Forschungsgemeinschaft SFB 566 and European funding from PIOF-GA-2008-221359 – Marie Curie Action.

Conflict of interest

None declared.

References

1. Hayden, M.S. and Ghosh, S. (2008) Shared principles in NF-kappaB signaling. *Cell* **132**, 344–362
2. Huxford, T. and Ghosh, G. (2009) A structural guide to proteins of the NF-kappaB signaling module. *Cold Spring Harb. Perspect. Biol.* **1**, a000075
3. Hoffmann, A., Natoli, G., and Ghosh, G. (2006) Transcriptional regulation via the NF-kappaB signaling module. *Oncogene* **25**, 6706–6716
4. Huang, D.B., Huxford, T., Chen, Y.Q., and Ghosh, G. (1997) The role of DNA in the mechanism of NFkappaB dimer formation: crystal structures of the dimerization domains of the p50 and p65 subunits. *Structure* **5**, 1427–1436
5. Ghosh, S., May, M.J., and Kopp, E.B. (1998) NF-kappa B and Rel proteins: evolutionarily conserved mediators of immune responses. *Annu. Rev. Immunol.* **16**, 225–260
6. Hayden, M.S. and Ghosh, S. (2004) Signaling to NF-kappaB. *Genes Dev.* **18**, 2195–2224
7. Nourbakhsh, M. and Hauser, H. (1999) Constitutive silencing of IFN-beta promoter is mediated by NRF (NF-kappaB-repressing factor), a nuclear inhibitor of NF-kappaB. *EMBO J.* **18**, 6415–6425
8. Nourbakhsh, M., Kalble, S., Dorrie, A., Hauser, H., Resch, K., and Kracht, M. (2001) The NF-kappa b repressing factor is involved in basal repression and interleukin (IL)-1-induced activation of IL-8 transcription by binding to a conserved NF-kappa b-flanking sequence element. *J. Biol. Chem.* **276**, 4501–4508
9. Dreikhausen, U., Hiebenthal-Millow, K., Bartels, M., Resch, K., and Nourbakhsh, M. (2005) NF-kappaB-repressing factor inhibits elongation of human immunodeficiency virus type 1 transcription by DRB sensitivity-inducing factor. *Mol. Cell. Biol.* **25**, 7473–7483
10. Lu, Z., Li, Y., Takwi, A., Li, B., Zhang, J., Conklin, D.J., Young, K.H., and Martin, R. (2011) miR-301a as an NF-kappaB activator in pancreatic cancer cells. *EMBO J.* **30**, 57–67
11. Ho, S.C., Lee, K.Y., Chan, Y.F., Kuo, L.W., Ito, K., Adcock, I.M., Chen, B.C., Sheu, J.R., Lin, C.H., and Kuo, H.P. (2009) Neutrophil elastase represses IL-8/CXCL8 synthesis in human airway smooth muscle cells through induction of NF-kappa B repressing factor. *J. Immunol.* **183**, 411–420
12. Bartels, M., Schweda, A.T., Dreikhausen, U., Frank, R., Resch, K., Beil, W., and Nourbakhsh, M. (2007) Peptide-mediated disruption of NFkappaB/NRF interaction inhibits IL-8 gene activation by IL-1 or Helicobacter pylori. *J. Immunol.* **179**, 7605–7613
13. Omnus, D.J., Mehrtens, S., Ritter, B., Resch, K., Yamada, M., Frank, R., Nourbakhsh, M., and Reboll, M.R. (2011) JKTBP1 is involved in stabilization and IRES-dependent translation of NRF mRNAs by binding to 5′ and 3′ untranslated regions. *J. Mol. Biol.* **407**, 492–504
14. Beutling, U., Stading, K., Stradal, T., and Frank, R. (2008) Large-scale analysis of protein-protein interactions using cellulose-bound peptide arrays. *Adv. Biochem. Eng. Biotechnol.* **110**, 115–152
15. Dikmans, A., Beutling, U., Schmeisser, E., Thiele, S., and Frank, R. (2006) SC2: a novel process for manufacturing multipurpose high-density chemical microarrays. *QSAR Comb. Sci.* **25**, 1069–1080
16. Sabe, H., Kondo, S., Shimizu, A., Tagaya, Y., Yodoi, J., Kobayashi, N., Hatanaka, M., Matsunami, N., Maeda, M., Noma, T. *et al.* (1984) Properties of human interleukin-2 receptors expressed on non-lymphoid cells by cDNA transfection. *Mol. Biol. Med.* **2**, 379–396
17. Rigaut, G., Shevchenko, A., Rutz, B., Wilm, M., Mann, M., and Seraphin, B. (1999) A generic protein purification method for protein complex characterization and proteome exploration. *Nat. Biotechnol.* **17**, 1030–1032
18. Formosa, T., Barry, J., Alberts, B.M., and Greenblatt, J. (1991) Using protein affinity chromatography to probe structure of protein machines. *Methods Enzymol.* **208**, 24–45
19. Niedick, I., Froese, N., Oumard, A., Mueller, P.P., Nourbakhsh, M., Hauser, H., and Koster, M. (2004)

Nucleolar localization and mobility analysis of the NF-kappaB repressing factor NRF. *J. Cell. Sci.* **117**, 3447–3458
20. Frank, R. (2002) The SPOT-synthesis technique. Synthetic peptide arrays on membrane supports–principles and applications. *J. Immunol. Methods* **267**, 13–26
21. Frank, R. (1992) Spot-synthesis: an easy technique for the positionally addressable, parallel chemical synthesis on a membrane support. *Tetrahedron* **48**, 9217–9232
22. Grilli, M., Chiu, J.J., and Lenardo, M.J. (1993) NF-kappa B and Rel: participants in a multiform transcriptional regulatory system. *Int. Rev. Cytol.* **143**, 1–62
23. Escalante, C.R., Shen, L., Thanos, D., and Aggarwal, A.K. (2002) Structure of NF-kappaB p50/p65 heterodimer bound to the PRDII DNA element from the interferon-beta promoter. *Structure* **10**, 383–391
24. Schmitz, M.L. and Baeuerle, P.A. (1991) The p65 subunit is responsible for the strong transcription activating potential of NF-kappa B. *EMBO J.* **10**, 3805–3817
25. Schmitz, M.L., Mattioli, I., Buss, H., and Kracht, M. (2004) NF-kappaB: a multifaceted transcription factor regulated at several levels. *Chembiochem.* **5**, 1348–1358
26. Hiroi, M. and Ohmori, Y. (2003) The transcriptional coactivator CREB-binding protein cooperates with STAT1 and NF-kappa B for synergistic transcriptional activation of the CXC ligand 9/monokine induced by interferon-gamma gene. *J. Biol. Chem.* **278**, 651–660
27. Schmitz, M.L., Stelzer, G., Altmann, H., Meisterernst, M., and Baeuerle, P.A. (1995) Interaction of the COOH-terminal transactivation domain of p65 NF-kappa B with TATA-binding protein, transcription factor IIB, and coactivators. *J. Biol. Chem.* **270**, 7219–7226
28. Chen, Y.Q., Ghosh, S., and Ghosh, G. (1998) A novel DNA recognition mode by the NF-kappa B p65 homodimer. *Nat. Struct. Biol.* **5**, 67–73
29. Ghosh, G., van Duyne, G., Ghosh, S., and Sigler, P.B. (1995) Structure of NF-kappa B p50 homodimer bound to a kappa B site. *Nature* **373**, 303–310
30. Karin, M., Yamamoto, Y., and Wang, Q.M. (2004) The IKK NF-kappa B system: a treasure trove for drug development. *Nat. Rev. Drug Discov.* **3**, 17–26
31. Tak, P.P. and Firestein, G.S. (2001) NF-kappaB: a key role in inflammatory diseases. *J. Clin. Invest.* **107**, 7–11
32. Schrodinger, L.L.C. (2010) The PyMOL Molecular Graphics System, Version 0.99.